J Mater Sci: Mater Electron (2013) 24:993–998
DOI 10.1007/s10854-012-0864-9

Optical absorption of radio frequency sputtered GaAs(Ti) films

A. Boronat · S. Silvestre · D. Fuertes Marrón · L. Castañer · A. Martí · A. Luque

Received: 12 June 2012 / Accepted: 3 August 2012 / Published online: 14 August 2012
© Springer Science+Business Media, LLC 2012

Abstract Composition and optical absorption of thin films of GaAs(Ti) and GaAs, deposited by sputtering on glass substrates under different process conditions, have been investigated. The thin films obtained are typically 200 nm thick. ToF–SIMS measurements show a quite constant concentration and good uniformity of Ti profiles along the GaAs(Ti) layers in all cases and EPMA results indicate that Ti content increases with the substrate temperature in the sputtering process. Measurements of the transmittance and reflectance spectra of the GaAs and GaAs(Ti) thin films have been carried out. In the optical characterization of the films it is found that optical absorption is enhanced in all samples containing Ti. The determination of the optical gap from the optical absorption, shows optical gap variations from 1.15 to 1.29 eV in the GaAs thin films, and from 0.83 to 1.13 eV in the GaAs(Ti) thin films. The differences in absorption and EgTAUC observed between samples of GaAs and GaAs(Ti) are consistent with the presence of an intermediate band.

1 Introduction

Quantum dots (QD's), have been proposed as one of the means to fabricate practical intermediate band (IB) solar cell [1–6]. InAs/GaAs QD's in GaAs bulk were investigated and sub-bandgap photocurrent was clearly proven by quantum efficiency measurements since the fabrication of the first IB solar cells [6]. Moreover, the concurrence of two below bandgap energy photons to generate one net electron–hole pair was also demonstrated [7]. However, the increase of current observed in these solar cells was small and an important voltage reduction was also observed in these devices. Weak absorption is one of the reasons contributing to the low efficiency of QD's IB solar cells [8].

In addition to QD's related devices, a range of different bulk materials have been proposed as candidates to IB materials for solar cell fabrication. High concentration of impurities producing deep levels in semiconductors may produce IB materials with reduced non-radiative recombination (NRR) [9]. These materials may support a higher density of IB states and therefore may lead to stronger sub-bandgap photon absorption.

In adittion, highly mismatched alloys (HMAs) (III–V and II–VI alloys, where a small amount of V or VI anions are replaced with the isovalent N and O respectively) have been investigated [10, 11]. IB solar cells have been fabricated using ZnTe:O alloys [11] and the grown of highly mismatched $ZnTe_{1-x}O_x$ alloys by molecular beam epitaxy have been described [12]. Moreover, in recent works IB photovoltaic solar cell based on GaN_xAs_{1-x} alloys has been also reported [13].

On the other hand, intermediate band materials based on $CuGaS_2$ chalcopyrite semiconductor have also been investigated and the potential of the thin film intermediate band solar cell (TF-IBSC) based on chalcopyrite absorbers has been evaluated [14–17].

Furthermore, interesting works have been carried out with silicon implanted with Ti. Silicon samples heavily doped with Ti have been prepared by ion implantation

A. Boronat · S. Silvestre (✉) · L. Castañer
MNT-Electronic Engineering Department, Universitat Politècnica de Catalunya, C/Jordi Girona 1-3, Campus Nord UPC, 08034 Barcelona, Spain
e-mail: santiago.silvestre@upc.edu

D. Fuertes Marrón · A. Martí · A. Luque
Instituto de Energía Solar, Universidad Politécnica de Madrid, ETSIT de Madrid, Ciudad Universitaria s/n, 28040 Madrid, Spain

followed by a pulsed-laser melting process [18, 19]. NRR suppression, when the deep level impurity exceeds the delocalization transition, has been observed in these samples [20]. The Ti-doped layer seems to show p-mobility, which is attributed to the almost electron-filled Ti level that would act as an IB [21].

Density functional theory (DFT) calculations have been applied to study main properties of III-nitrides GaN and InN, and $In_xGa_{1-x}N$ solid solutions, that present tunable band gap energy [22], and also to study a number of ternary solid solutions including $Ti_xGa_nAs_m$ [23]. In some of these works, ab initio band calculations have suggested that certain transition metals could form an IB in III–V compounds [23–25] GaAs(M), GaP(M), where M is a transition Metal : Z, Sc, Ti, V, Cr, Mn, Fe, Co, Ni, Cu and Zn. These compounds have been also proposed as candidates to IB bulk materials. In this respect, we have been studying the properties of Galium_arsenide (Titanium implanted), GaAs(Ti), as candidate IB material [26, 27]. In these previous works we reported absorbance peaks, around 1.3 and 1.7 eV, in samples of n_GaAs whit thin films of GaAs(Ti) on its surface [27]. In the present work we report results obtained in optical characterization of GaAs(Ti) and GaAs thin films deposited by sputtering on glass substrates.

2 Materials and methods

Thin films of GaAs(Ti) and GaAs, with thickness ranging from 90 to 250 nm, were deposited by sputtering at different conditions, using an ESM100 Edwards & RFS5 Generator-300 W sputtering system. Although most of the samples we have used for measurements are typically 200 nm thick.

Two different targets have been used in these processes:

- A target of n_GaAs <100> having a Si impurity concentration of 7×10^{17} cm^{-3}, with a diameter of 4″.
- A target of GaAsTi : GaAs (99.5 %)–Ti (0.5 %), Purity; 99,999 %, with a diameter of 4″.

The sputter conditions of the processes were: (1) chamber pressure 5 10^{-1} Pa; (2) Ar flux 5, 10, and 15 sccm. (3) The R.F. input power was ranging from 16 to 40 W. (4) Substrate temperatures ranging from 30 to 400 °C. (5) Target-to-substrate distance 6.5 cm. (6) Depositions were made without sample rotation.

Table 1 summarizes the R.F. input power, Ar flux and substrate temperature used in the sputtering processes for each sample.

Photoreflectance (PR) measurements were carried out at room temperature by measuring direct reflectance of the samples upon monochromatic illumination with a 150 W halogen lamp, using a 325 nm (He–Cd, 15 mW) laser beam chopped at 777 Hz as modulating agent and a Ge detector. Further details of the set-up can be found elsewhere [28].

Table 1 Sputtering process conditions

Sample	RF power (W)	T (°C)	Ar flux (sccm)
GaAs(Ti)1	16	200	10
GaAs(Ti)2	20	390	10
GaAs(Ti)3	32	200	10
GaAs(Ti)4	40	390	10
GaAs1	25	30	15
GaAs2	25	200	10
GaAs3	28	400	5

The composition of the films obtained has been analyzed by ToF–SIMS and electron probe micro-analyzer (EPMA) measurements. Xray diffraction (XRD) was used to analyse the structure of the deposited thin films. The XRD measurements were made using a Philips MRD diffractometer. Measurements of the transmittance, T, and reflectance, R, spectra of the GaAs and GaAs(Ti) thin films were obtained using a Shimadzu UV-3600 UV–VIS-NIR spectrophotometer in the visible and near infrared ranges.

3 Results and discussion

3.1 Composition and structural properties

The structural and electrical properties of sputtered GaAs films are mainly governed by process conditions during the film deposition [29–31]. Amorphous structure of thin films of GaAs deposited by RF sputtering at substrate temperatures below 50 °C has been reported, and is known that an increase of the substrate temperature favours crystallization. This amorphous structure tends to disappear at substrate temperatures up to 500 °C [29], but the excess of As present on the films plays an important role on its structure and optical properties [31]. The maximum substrate temperature used in this study was 400 °C, although partial recrystallization has been also observed in some of these samples. However, the reason why we did not try with temperatures above 400 °C is to prevent the IB, if it exists, to disappear as has been suggested in the recent works [18–21], were it has been shown that Silicon samples heavily doped with Ti have shown IB characterisitics, and the estability of this IB strongly depends on the annealing temperature of these samples [32]. The electrical behavior of these Si samples implanted at high doses of Ti has been reported as fairly unstable, even using annealing temperatures as low as 200° C the effective electronic transport properties of these bilayers are modified. So, we did not use temperatures beyond 400° C in this work.

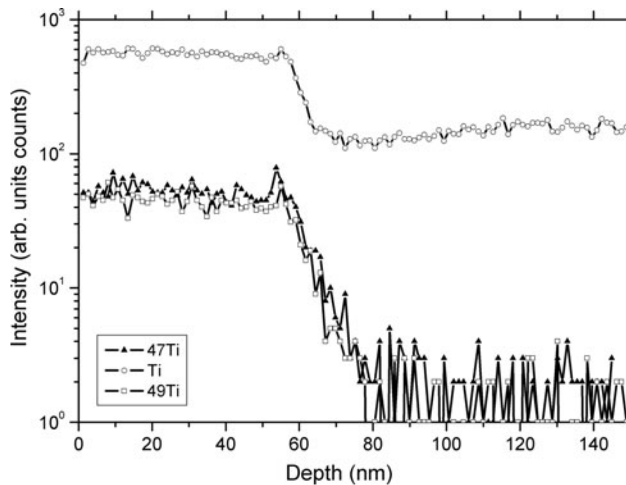

Fig. 1 Tof–SIMS of GaAsTi on glass substrate

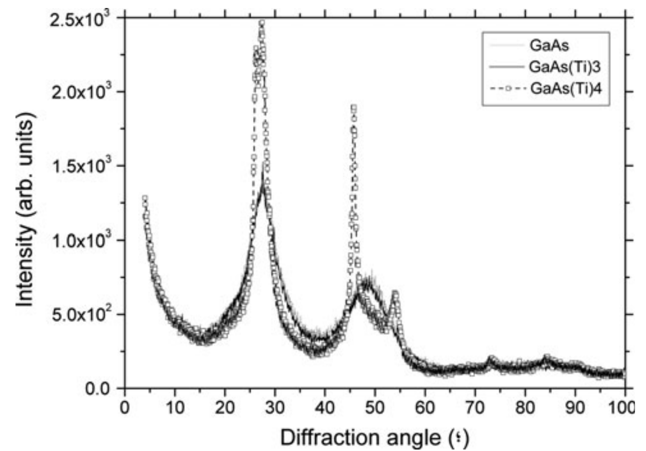

Fig. 2 X-ray diffraction measurement results

Tof–SIMS measurements were carried out in all samples deposited. A quite constant concentration and very good uniformity of Ti profiles were observed along the GaAs(Ti) layers in all cases. Figure 1 shows Tof–SIMS results obtained for a GaAs(Ti) sample deposited on glass using a RF power of 16 W and 200 °C of substrate temperature. The differences in composition of GaAs(Ti) samples fabricated, analyzed by EPMA, are shown in Table 2. The samples present relevant Ti content, and this behaviour increases with temperature.

The results obtained from XRD measurements of the deposited layers have shown dominant amorphous structure for samples deposited at substrate temperatures of 200 °C or below this value. Partial recrystallization has been observed for samples deposited at substrate temperatures around 400 °C, as can be seen in Fig. 2 where some peaks at 27.5° and 45.4°, corresponding to (111) planes of c-GaAs and GaAs (220) planes respectively, appear. Furthermore, a peak at 53.7° associated to GaAs (311) is also observed.

3.2 Optical properties

The absorption coefficient α in the strong absorption region was used to determine the optical energy gap of the samples. The absorption coefficient was evaluated from the following relation:

$$T = (1 - R)e^{-(\alpha d)} \quad (1)$$

where d is the thickness of the deposited thin layers, measured using a perfilometer Veeco Dekktak.

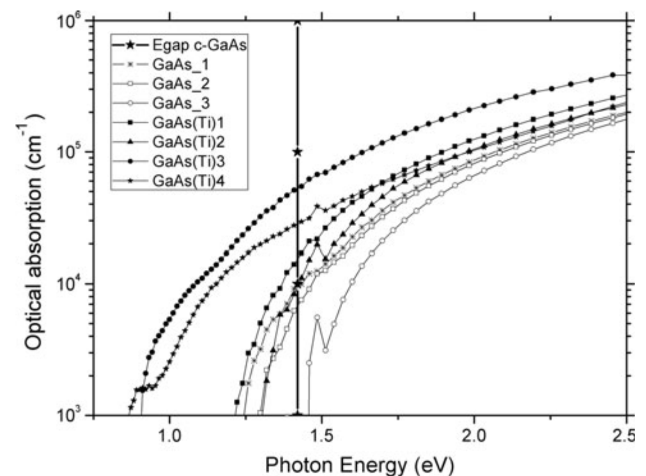

Fig. 3 Optical absorption from Eq. (1)

The optical absorption of the samples is influenced by the sputtering process conditions: RF power, substrate temperature and other desposition conditions that directly affect the crystal quality of the sputter-deposited films. The Ti-inclusions have also important effects in the absorption of these films. The optical absorption is enhanced by the presence of Ti in all cases. This behaviour has been observed in all samples fabricated with independence of the sputtering process conditions used, as can be seen in Fig. 3.

The effect of substrate temperature, in Figs. 3 and 4, does not explain alone such changes that we interpret as, at least partially, due to the Titanium content. Furthermore the RF power used in the sputtering process of samples

Table 2 EPMA Results obtained

Sample	Temperature of deposition (°C)	W %(Ga)	W %(As)	W %(Ti)	A %(Ga)	A %(As)	A %(Ti)
GaAs(Ti)1	200	48.76	51.06	0.18	50.51	49.22	0.27
GaAs(Ti)2	390	48.92	50.89	0.19	50.67	49.05	0.28

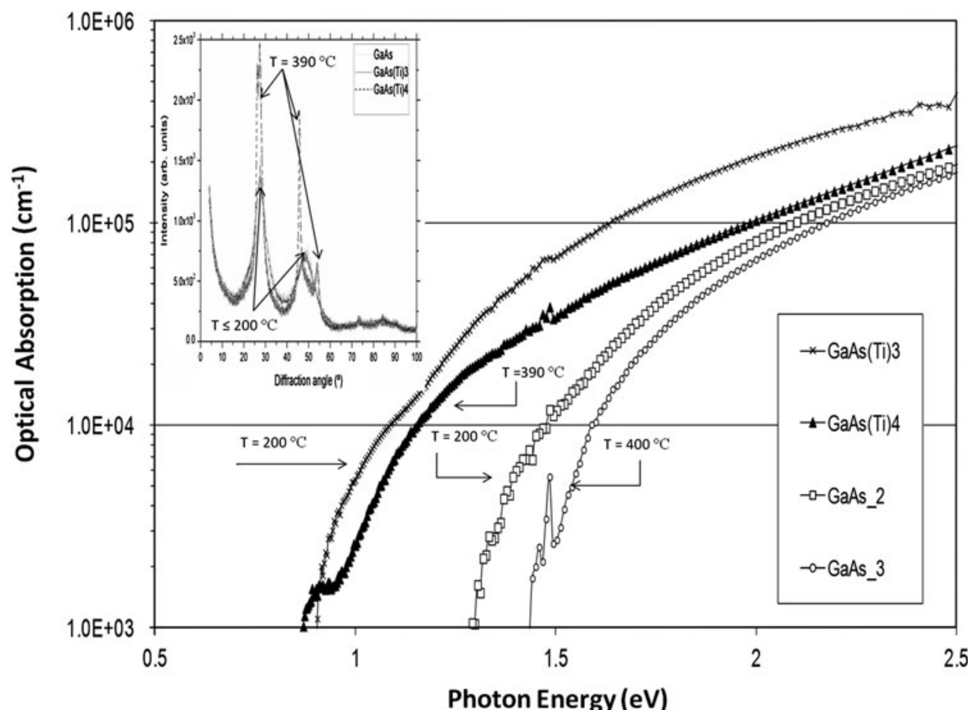

Fig. 4 Optical absorption

GaAs(Ti)3, GaAs2 and GaAs3 is not so different to introduce important changes in crystallinity.

In the Fig. 4 inset, we show that for substrate temperatures in the range of 400° C the crystallinity is quite good whereas for temperatures of 200° C or lower the films have more amorphous nature. Again only changes in crystallinity do not explain the absorption changes we have observed by incorporating Ti to GaAs.

For the determination of the optical gap, we have used the approach of Tauc [33–35]. We have made a least-square fit to the experimental data using the following equation:

$$(\alpha h\nu)^{1/2} = C_{\mathrm{TAUC}}(h\nu - E_{\mathrm{gTAUC}}) \quad (2)$$

where h is Planck's constant, C_{TAUC} is the slope of the TAUC extrapolation and E_{gTAUC} represents the corresponding TAUC optical gap.

The optical energy gap values were obtained by extrapolating the linear range of the plots of $(\alpha h\nu)^{1/2}$ versus $h\nu$ to $\alpha = 0$, as shown in Fig. 5 below. In this analysis, we perform our fit of Eq. (2) to the experimental data for which $5.03 \times 10^4\ \mathrm{cm}^{-1} < \alpha < 9.96 \times 10^5\ \mathrm{cm}^{-1}$. In Table 3, the fits of Eq. (2), corresponding to the GaAs(Ti) and GaAs samples are tabulated. The lower and the upper fit limits of α used in the fits are specified in the table, as well as the values obtained for C_{TAUC} and E_{gTAUC} for all samples. It was observed that the corresponding E_{gTAUC} varied from 1.15 to 1.29 eV in GaAs samples, and from 0.83 to 1.13 eV in GaAs(Ti) samples.

The differences in absorption and E_{gTAUC} observed between samples of GaAs and GaAs(Ti) are in agreement

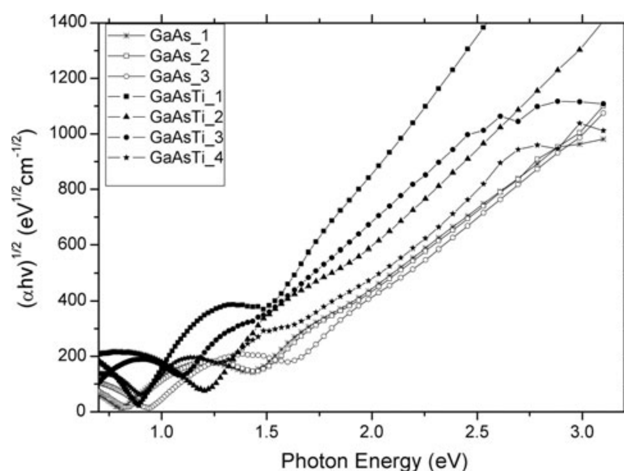

Fig. 5 TAUC plot

with theoretical predictions for IB formation in this kind of compounds [23, 24], and are consistent with the presence of an IB, stable and with metallic character, formed between the valence band and the conduction band in samples having Ti content.

An isolated intermediate band can be found when Ti atoms replace substitutionally As atoms in the crystal, then values from 0.86 to 1.08 eV, for the intermediate bandwidth (ΔEI), have been predicted for Ga_4As_3Ti [24]. Our interpretation of the EPMA results is that these values are very similar to the values obtained in the samples, especially in the case of samples having more Ti content. It is not possible to conclude, however, whether this band is

Table 3 Values for optical energy gap calculation

Sample	EgTAUC (eV)	CTAUC ($cm^{-1/2}eV^{-1/2}$)	$\alpha(cm^{-1})$ Lower	Upper
GaAs(Ti)1	1.12	982.86	2.6×10^5	9.96×10^5
GaAs(Ti)2	1.13	695.7	1.38×10^5	5.68×10^5
GaAs(Ti)3	0.99	679.55	1.71×10^5	3.47×10^5
GaAs(Ti)4	0.83	405.46	8.72×10^4	2.55×10^5
GaAs1	1.15	538.04	1.4×10^5	3.11×10^5
GaAs2	1.23	574.35	6.62×10^4	3.38×10^5
GaAs3	1.29	581.97	5.03×10^4	3.26×10^5

isolated or connected to the conduction band by a null density of states or not.

Figure 6 shows the recorded PR-spectra obtained from the GaAs and GaAs(Ti) samples. The reference GaAs samples, seem to show a weak and rather broad PR-signature around 1.4 eV, which would speak of residual crystallization. The signal is too weak as to draw any conclusion from any attempt to fit the spectra according to the third-derivative model of Aspnes [36].

Additionally, the range below 0.9 eV should not be considered as representative due to the poor signal-to-noise

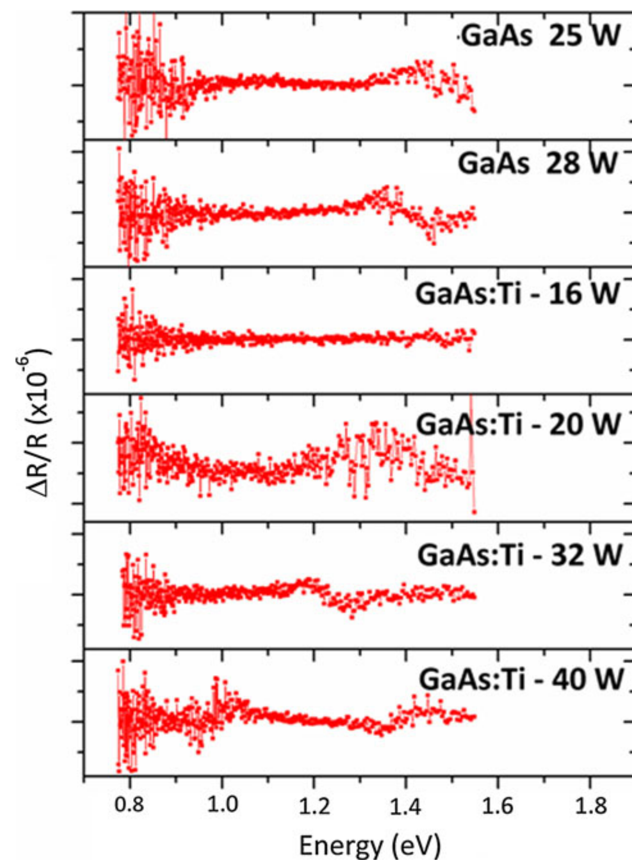

Fig. 6 Photoreflectance spectra of n-GaAs and GaAs(Ti) samples

ratio obtained. Notwithstanding, slight differences in the line shape between both samples could be interpreted in terms of a marginally better crystallization in the case of the sample grown at 28 W and substrate temperature of 400 °C, accordly with results obatined from XRD measurements on samples deposited at the same temperature. Concerning the Ti-containing samples, the one grown at 16 W and substrate temperature of 200 °C is PR-silent. Increasing the power to 20 W and the substrate temperature to 390 °C leads to the recovery of the broad and weak signal around 1.4 eV, which in our interpretation would correspond to the power and temperature thresholds required as to achieve a noticeable degree of crystallinity in the samples.

The sample grown at 32 W and substrate temperature of 200 °C presents a PR-signature red shifted down to about 1.2 eV, with no further evidence of the signal at 1.4 eV. The sample grown at 40 W and substrate temperature of 390 °C shows two apparent signatures; one at about 1.4 eV and a second one slightly above 1.0 eV.

The energies of the lowest critical points of sample grown at 32 W and substrate temperature of 200 °C, and ample grown at 40 W and substrate temperature of 390 °C, detected from PR (Fig. 6) do not correspond to the absorption edges obtained from R and T (Fig. 3, Table 3). Such a difference is tentatively attributed to the dominant contribution of amorphous phases to the band edges, with minor contributions of crystalline domains only at slightly higher energies. The eventual indirect nature of the fundamental absorption threshold in Ti-containing samples, which could also explain its PR-silent character, appears much less likely.

4 Conclusion

Thin films of GaAs(Ti) and GaAs have been deposited by sputtering on glass substrates under different process conditions. ToF–SIMS measurements confirm that Ti profiles show good uniformity and constant concentration along the layers deposited in all cases.

The composition of GaAs(Ti) samples fabricated has been analyzed by EPMA. The samples present relevant Ti content, and this behavior increases with the temperature of the samples along the sputtering process.

Optical absorption is enhanced in all samples containing Ti. The optical gap varies from 1.15 to 1.29 eV in the GaAs thin films while it varies from 0.83 to 1.13 eV in the GaAs(Ti) thin films.

The results obtained from XRD measurements of the deposited layers have shown dominant amorphous structure for samples deposited at substrate temperatures of 200 °C or below this value and partial recrystallization for

samples deposited at substrate temperatures around 400 °C.

Photoreflectance results reveal a marginal degree of crystallinity for samples grown at a power of 20 W or more, especially in GaAsTi samples deposited at temperatures of 390 °C, and the presence of additional signatures in Ti-containing samples at energies slightly higher than the corresponding absorption thresholds.

The differences in absorption and EgTAUC observed between samples of GaAs and GaAs(Ti) are consistent with the presence of an intermediate band. It is not possible to conclude, however, whether this band is isolated or connected to the conduction band by a null density of states or not.

Acknowledgments This work is partially supported by The Spanish Ministry of Education and Science under Consolider Ingenio 2010 Program, through the project GENESIS-FV (CSD2006-0004).

References

1. A. Luque, A. Martí, C. Stanley, Nat. Photonics **6**, 146 (2012)
2. A. Luque, A. Martí, Phys. Rev. Lett. **78**, 5014 (1997)
3. L. Cuadra, A. Martí, A. Luque, Thin Solid Films **451–452**, 593 (2004)
4. A. Martí, N. López, E. Antolín, E. Cánovas, C. Stanley, C. Farmer, L. Cuadra, A. Luque, Thin Solid Films **511–512**, 638 (2006)
5. E. Antolín, E. Martí, C.R. Stanley, C.D. Farmer, E. Cánovas, N. López, P.G. Linares, A. Luque, Thin Solid Films **516**, 6919 (2008)
6. A. Luque, A. Martí, C. Stanley, N. López, L. Cuadra, D. Zhou, J.L. Pearson, A. McKee, J. Appl. Phys. **96**, 903 (2004)
7. A. Martí, E. Antolin, C.R. Stanley, C.D. Farmer, N. López, P. Díaz, E. Canovas, P.G. Linares, A. Luque, Phys. Rev. Lett. **97**, 2477014 (2006)
8. A. Luque, A. Martí, Nat. Photonics **5**, 137 (2011)
9. A. Luque, A. Martí, E. Antolín, C. Tablero, Phys. B **382**, 320 (2006)
10. K.M. Yu, W. Walukiewicz, J. Wu, W. Shan, J.W. Beeman, M.A. Scarpulla, O.D. Dubon, P. Becla, Phys. Rev. Lett. **91**, 246403 (2003)
11. W. Wang, S. Lin Albert, J.D. Phillips, Appl. Phys. Lett. **95**, 011103 (2009)
12. T. Tanaka, S. Kusaba, T. Mochinaga, K. Saito, Q. Guo, M. Nishio, M. Yu Kin, W. Walukiewicz, Appl. Phys. Lett. **100**, 011905-1–011905-3 (2012)
13. N. López, L.A. Reichertz, K.M. Yu, K. Campman, W. Walukiewic, Phys. Rev. Lett. **106**, 028701 (2011)
14. Y. Seminóvski, P. Palacios, P. Wahnón, Thin Solid Films **519**, 7517 (2011)
15. I. Aguilera, P. Palacios, P. Wahnón, Thin Solid Films **516**, 7055 (2008)
16. D. Fuertes Marrón, A. Martí, A. Luque, Thin Solid Films **517**, 2452 (2009)
17. A. Martí, D. Fuertes Marrón, A. Luque, J. Appl. Phys. **103**, 073706 (2008)
18. J. Olea, M. Toledano-Luque, D. Pastor, G. González-Díaz, I. Mártil, J. Appl. Phys. **104**, 016105 (2008)
19. D. Pastor, J. Olea, A. Del Prado, G. Garcia-Hemme, I. Martil, G. Gonzalez-Dıaz, J. Ibañez, R. Cusco, L. Artús, Semicond. Sci. Technol. **26**, 115003 (2011)
20. E. Antolin, A. Martí, J. Olea, D. Pastor, G. Gonzalez-Diaz, I. Martíl, A. Luque, Appl. Phys. Lett. **94**, 042115 (2009)
21. G. Gonzalez-Díaz, J. Olea, I. Mártil, D. Pastor, A. Martí, E. Antolín, A. Luque, Sol. Energy Mater. Sol. Cells **93**, 1668 (2009)
22. L. Dong, S.P. Alpay, J. Mater. Sci. (2012). doi:10.1007/s10853-012-6351-0
23. P. Whanón, P. Palacios, J.J. Fernández, C. Tablero, J. Mater. Sci. **40**, 1383 (2005). doi:10.1007/s10853-005-0570-6
24. P. Wahnón, C. Tablero, Phys. Rev. B. **65**, 165115 (2002)
25. C. Tablero, Solid State Commun. **133**, 97 (2005)
26. S. Silvestre, J. Puigdollers, A. Boronat, L. Castañer, Analysis of GaAs-Ti thin films deposited by sputtering onto c-Si and GaAs. Presented at the 7th IEEE Spanish conference on electron devices, Santiago de Compostela, Spain, 19–24 February 2009
27. S. Silvestre, A. Boronat, L. Castañer, D. Fuertes Marrón, A. Martí, A. Luque, Study of GaAs(Ti) thin films as candidates for IB solar cells manufacturing. Presented at the 35th IEEE photovoltaic specialists conference, Honolulu, Hawaii, 20–25 June 2010
28. E. Cánovas, A. Martí, N. López, E. Antolín, P.G. Linares, C.D. Farmer, C.R. Stanley, A. Luque, Thin Solid Films **516**, 6943 (2008)
29. B. El Hadadi, R. Lbibb, A. Slaoui, Vacuum **83**, 1100 (2009)
30. B. El Hadadi, H. Carchano, J.-L. Seguin, H. Tijani, Vacuum **80**, 272 (2005)
31. K. Sedeek, J. Phys. D Appl. Phys. **26**, 130 (1993)
32. J. Olea, D. Pastor, I. Mártil, G. González-Díaz, Sol. Energy Mater. Sol. Cells **94**, 1907 (2010)
33. M.I. Manssor, E.A. Davis, J. Phys.: Condens. Matter **2**, 8063 (1990)
34. J. Tauc, R. Grigorovici, A. Vancu, Phys. Status Solidi **15**, 627 (1966)
35. J.H. Dias da Silva, R.R. Campomanes, D.M.G. Leite, J. Appl. Phys. **96**, 7052 (2004)
36. D.E. Aspnes, Surf. Sci. **37**, 418 (1973)